

Threshold stress in dispersionally strengthened superplastic Al alloys

N. Q. CHINH, A. JUHÁSZ, P. TASNÁDI, I. KOVÁCS

Institute for General Physics, Loránd Eötvös University, V, Egyetem-tér 1-3, 1364 Budapest, Hungary

It is important for practical applications that some commercial alloys with stabilized fine-grained structure should exhibit superplastic behaviour at high temperatures. In this paper the results of impression creep tests conducted on AlMgZn alloys are reported and the strain rate sensitivity and activation enthalpy were determined. The mechanical behaviour of the alloys as a function of the strain rate sensitivity can be divided into three regions. At low and high stresses the strain rate sensitivity parameter is low and the deformation process is not superplastic. Superplastic deformation takes place only at intermediate stresses. The microstructural interpretation of these processes involves, in general, the change of the micromechanisms controlling the different deformation processes. It was determined that by the supposition of a threshold stress depending strongly on temperature, the two regions due to low and intermediate stresses of the deformation can be described by the same constitutive equation.

1. Introduction

The high-temperature creep rate, $\dot{\epsilon}$, of pure metals and alloys can be described by the formula:

$$\dot{\epsilon} = A\sigma^{n_a} e^{-Q/kT} \quad (1)$$

where σ is the applied stress, A is a material parameter, n_a is the apparent stress exponent and Q_a is the apparent activation enthalpy [1, 2]. According to empirical evidence, A depends on the grain size and in some cases on temperature. The stress exponent, n , varies between 1 and 12 depending on the material, the strain rate and the temperature [3]. Using Equation 1 the stress exponent and the apparent activation energy can be determined experimentally using the equations

$$n_a = \left(\frac{\partial \ln \dot{\epsilon}}{\partial \ln \sigma} \right)_T \quad (2)$$

$$Q_a = -k \left(\frac{\partial \ln \dot{\epsilon}}{\partial (1/T)} \right)_{\sigma, n} \quad (3)$$

If the apparent activation enthalpy obtained experimentally agrees well with the enthalpy of a characteristic microstructural process (for example bulk or grain-boundary diffusion), then one can draw conclusions for the micromechanism of deformation. However, in some cases a more realistic stress exponent and activation enthalpy can be obtained if the creep process is described in terms of an effective stress, σ_e , which is the difference between the applied stress, σ , and a threshold stress, σ_0

$$\dot{\epsilon} = A(\sigma - \sigma_0)^n e^{-Q/kT} \quad (4)$$

This concept was originally applied for the description of creep processes in dispersionally strengthened alloys [4]. McLean [3] showed that if there is a strongly temperature dependent threshold stress, the apparent stress exponent and the apparent activation enthalpy

obtained experimentally differ significantly from the true values. Taking the threshold stress in the form

$$\sigma_0 = B e^{Q/kT} \quad (5)$$

it can be shown that the apparent stress exponent is related to n in Equation 4 by

$$n_a = \frac{n}{1 - (\sigma_0 - \sigma)} \quad (6)$$

Similarly, there is a simple relationship between the apparent activation enthalpy, Q_a , and the enthalpy, Q

$$Q_a = Q + \frac{nQ_0}{(\sigma/\sigma_0) - 1} \quad (7)$$

and also of superplastic flow. Superplastic materials can be deformed up to several hundred or a thousand per cent strains [5]. The superplastic deformation takes place at high temperature (above half of the absolute melting temperature) and at low strain rate (between 10^{-2} and 10^{-5} sec^{-1}). It is well known that the curve of the $\ln \sigma - \ln \dot{\epsilon}$ plot is sigmoidal and consists of three parts with a low value of n_a in the intermediate Region II, and high values of n_a in Regions I and III (Fig. 1). The real superplastic processes with extremely high elongations belong to Region II. In this region, n varies between 1 and 3 [6]. The lower limit ($n_a = 1$) corresponds to the ideal Newtonian flow which does not take place in real metallic materials. For some special fine-grained alloys, n_a is between 1 and 2. (These materials exhibit extremely high superplastic elongations.) In the case of commercial superplastic alloys, the stress exponent is between 2 and 3. The superplastic behaviour is characterized in general by the inverse of the stress exponent, which is the strain rate sensitivity

$$m = \frac{1}{n} = \left. \frac{\partial \ln \sigma}{\partial \ln \dot{\epsilon}} \right|_T \quad (8)$$

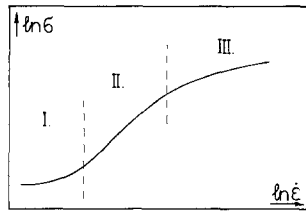


Figure 1 Schematic illustration of the stages of deformation as a function of strain rate.

A deformation process can be considered as superplastic if $m > 0.3$. Outside the optimal strain rate and temperature range (regions I and III), m becomes less than 0.3 and in general the activation enthalpy is higher than that of the superplastic process. It is a general assumption that different deformation mechanisms are working in the three regions. In the first and third regions the controlling mechanism of the process is probably the bulk diffusion while in the second region grain-boundary sliding dominates.

Recently, Mohamed suggested a new interpretation for the mechanical behaviour of two superplastic alloys (Zn–22% Al and Pb–62% Sn) [7]. Assuming a strongly temperature-dependent threshold stress, Mohamed showed that the deformation behaviour of these alloys in the first two regions can be explained without supposing a change in the deformation mechanism. In this case the apparent stress exponent and the activation enthalpy change due to the temperature-dependent threshold stress. Mohamed showed that the true activation enthalpy is lower than that obtained experimentally, and it agrees well with that of the grain-boundary diffusion.

The experimental results obtained by impression creep tests on superplastic AlMgZn alloys are reported here and are interpreted assuming a temperature-dependent threshold stress. However, it was found that both the apparent and true activation enthalpy remain higher than that of the bulk diffusion.

2. Experimental procedure

The chemical composition of the alloys investigated is given in Table I. The alloys were prepared from 99.99% purity aluminium by Hungalu Engineering and Development Centre, Budapest. After casting the alloys were annealed at 480°C for 3 h and at 400°C for 8 h. After this the cast rods were hot rolled and finally annealed at 480°C for 0.5 h during which the material was recrystallized.

The alloys were investigated by impression creep tests at different loads and temperatures. The tests were carried out with a home-made device the details of which were published earlier [8]. The measurements were performed in the temperature range 440 to 570°C.

In the impression creep test a cylindrical flat-ended punch is pressed continuously into the surface of

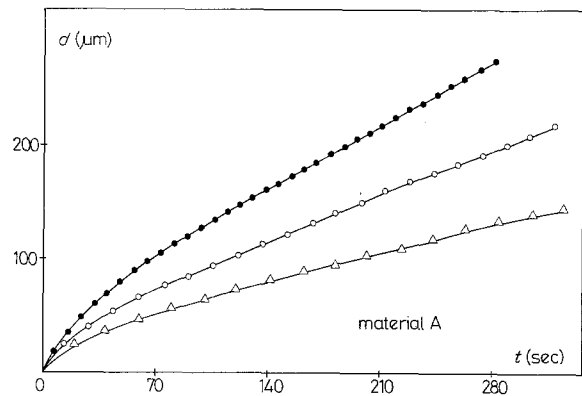


Figure 2 Impression depth as a function of time at different loads for material A, at 796 K. (●) $v = 0.75 \times 10^{-3} \text{ mm sec}^{-1}$, $P = 30.88 \text{ N mm}^{-2}$; (○) $v = 0.53 \times 10^{-3} \text{ mm sec}^{-1}$, $P = 25.03 \text{ N mm}^{-2}$; (Δ) $v = 0.34 \times 10^{-3} \text{ mm sec}^{-1}$, $P = 18.92 \text{ N mm}^{-2}$.

the sample. According to experimental evidence the velocity of the punch after a short time becomes constant and it can be given by the formula

$$v = C e^{-Q/kT} \quad (9)$$

where the pre-exponential factor, C , depends on the pressure, P , just below the punch as

$$C = C_0 P^n \quad (10)$$

where C_0 and n are constants. Both theoretical and experimental evidence exist that in order to compare this test with the tensile one the impression data must be converted to equivalent stresses and equivalent strain rates by the formulae

$$\begin{aligned} \sigma_{\text{eq}} &= \frac{P}{3} \\ \dot{\epsilon}_{\text{eq}} &= \frac{v}{d} \end{aligned} \quad (11)$$

where d is the diameter of the punch. It is important that the validity of these relationships is independent of the properties of the sample investigated. They can be equally used for single crystalline materials and for polycrystalline materials which have an average grain size much less than the diameter of the punch [9, 10].

3. Results and discussion

3.1. Determination of the strain rate sensitivity from impression creep curves

Fig. 2 shows characteristic creep curves of material A which were taken at various loads at $T = 796 \text{ K}$. Creep curves taken at various temperatures and at constant pressure ($P = 30.5 \text{ N mm}^{-1}$) are shown in Fig. 3. In the steady state part of the curves, the velocity of the punch is constant and it depends on the temperature and pressure. Figs 4 and 5 show the connection between the pressure and the equivalent strain rate for materials A and B, respectively. (Each

TABLE I Chemical composition of the alloys (wt %)

Alloy	Mg	Zn	Cu	Si	Cr	Fe	Zr	Mn	Ti
A	1.92	5.45	1.3	–	0.25	0.11	0.28	–	–
B	1.4	–	1.0	1.0	0.4	0.5	–	0.6	0.1

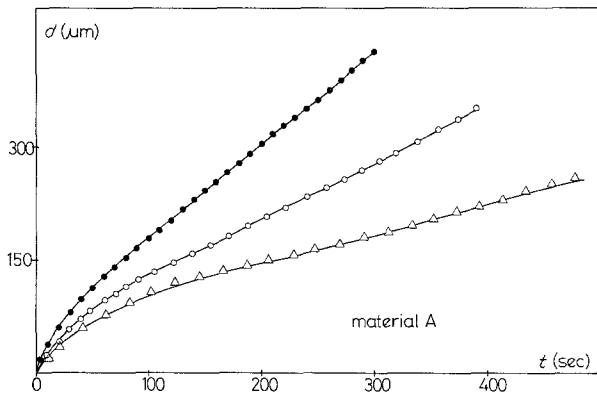


Figure 3 Impression depth as a function of time at different temperatures for material A, at $P = 30.5 \text{ N mm}^{-2}$. (●) $v = 1.65 \times 10^{-3} \text{ mm sec}^{-1}$, 816 K; (○) $v = 0.76 \times 10^{-3} \text{ mm sec}^{-1}$, 796 K; (Δ) $v = 0.33 \times 10^{-3} \text{ mm sec}^{-1}$, 778 K.

point is given by an average of three to five measured values.)

For material A at constant temperature, the $\ln P$ - $\ln v$ points fit a straight line, the slope of which gives the strain rate sensitivity parameter

$$m = \left(\frac{\partial \ln \sigma}{\partial \ln \dot{\epsilon}} \right)_T = \left(\frac{\partial \ln P}{\partial \ln v} \right)_T \quad (12)$$

The results obtained for material A show that above 500°C the strain rate sensitivity is higher than 0.3 so the deformation process can be regarded as superplastic (Fig. 4). For material B these points lie on characteristic sigmoidal curves (Fig. 5). The highest m values belong to the central part of these curves.

To determine the threshold stresses, stress was plotted as a function of $\dot{\epsilon}^m$. The result is shown in Figs 6 and 7 for materials A and B, respectively. Naturally the exponent m in this case must be chosen so that the measured points fit the straight lines, therefore m does not necessarily agree with that obtained from Equation 1. It was found that a suitable exponent was 0.5 and 0.45 for materials A and B, respectively. It can be seen from Equation 1 that the threshold stresses are given by extrapolation of the straight lines obtained, to $\dot{\epsilon} = 0$. Plotting $\ln \sigma_0$ against $1/T$ for materials A and B, straight lines are obtained (Figs 8 and 9). From the slope of these lines 50 and 82 kJ mol^{-1} were obtained for the activation enthalpy

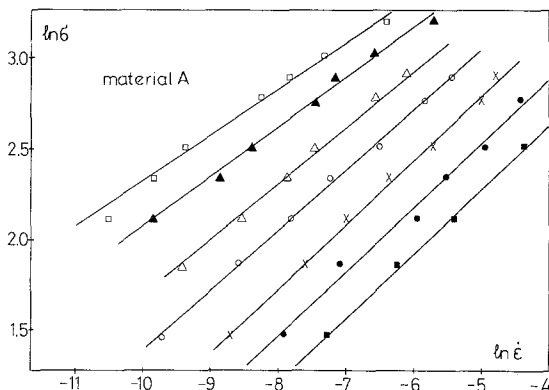


Figure 4 The connection between pressure and strain rate for material A. $T =$ (□) 738, (▲) 755, (Δ) 778, (○) 796, (x) 816, (●) 833, (■) 848 K.

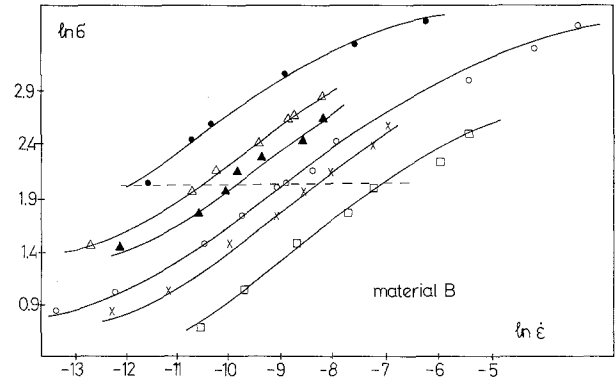


Figure 5 The connection between pressure and strain rate for material B. $T =$ (●) 759, (Δ) 773, (▲) 785, (○) 803, (x) 818, (□) 840 K.

connected with the threshold stress for materials A and B, respectively.

Taking into account the threshold stress and using an $\ln(\sigma - \sigma_0)$ - $\ln \dot{\epsilon}$ plot, a straight line with a slope of 0.45 can be obtained (Fig. 10) for Regions I and II in Fig. 1. The results show that the apparent strain rate sensitivities determined from the curves in Figs 4 and 5 are lower than the true value obtained in Fig. 10, but the deviation decreases with increasing pressure.

Strain rate sensitivities were also determined by the strain rate change method. The values obtained by this method are in approximate agreement with the true strain rate sensitivity.

3.2. The activation enthalpy of deformation

The apparent activation enthalpy of the deformation is determined from Equation 3. Using the cross-cut method, the readings of the creep curves taken at different temperatures (Figs 5 and 6) were replotted as $\ln \dot{\epsilon} - 1/T$ functions at constant σ (Figs 11 and 12). The apparent activation enthalpy can be calculated from the slope of these curves. Using Equations 6 and 7 the following simple relationship can be obtained between the apparent and true activation enthalpies

$$Q_a = (n_a - n)Q_0 + Q \quad (13)$$

This equation shows that the higher the deviation between the apparent stress exponent and the true one, the higher is the difference between the apparent

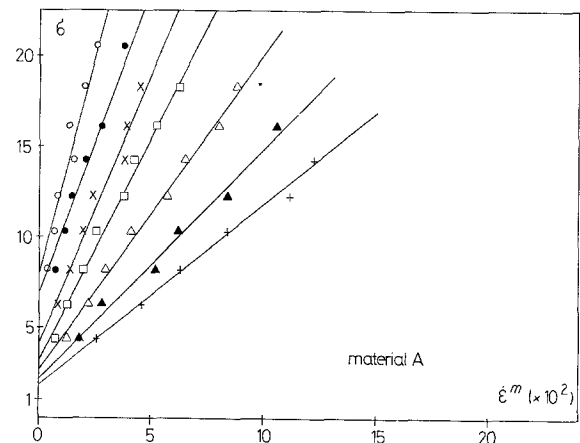


Figure 6 σ - $\dot{\epsilon}^m$ curves for material A; $m = 0.5$, $T =$ (○) 738, (●) 755, (x) 778, (□) 796, (Δ) 816, (▲) 833, (+) 848 K.

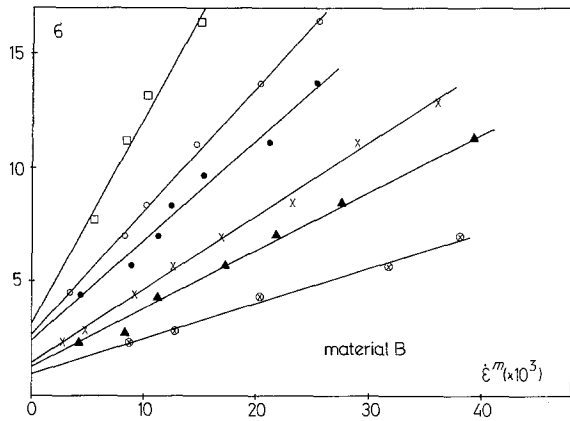


Figure 7 $\sigma - \epsilon^m$ curves for material B; $m = 0.45$, $T = (\square)$ 759, (\circ) 773, (\bullet) 785, (\times) 803, (\blacktriangle) 818, (\otimes) 840 K.

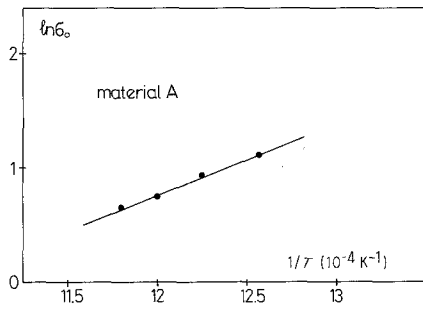


Figure 8 Determination of the activation energy of the threshold stress (material A). $Q_0 = 50 \text{ kJ mol}^{-1}$.

and true activation enthalpies. It can be seen, however, that in Regions I and II the apparent activation enthalpy tends to the true value with increasing applied stress. Replacing the apparent and true stress exponent ($n_a = 2.86$, $n = 2.7$) as well as the activation enthalpy of the threshold stress ($Q_a = 50 \text{ kJ mol}^{-1}$, $Q = 82 \text{ kJ mol}^{-1}$) in Equation 13 the values $Q = 177$ and 253 kJ mol^{-1} are obtained as true activation enthalpies for materials A and B, respectively. It can be seen that these values are rather higher than the self diffusion energy of aluminium.

Experimental evidence exists that the activation enthalpy of the superplastic processes in eutectic Pn-Sn and eutectoid Zn-Al alloys agrees with that of the grain-boundary diffusion [11, 12]. Previously the same results were obtained for an AlZnMg alloy grain-refined by zirconium [13]. At the same time the

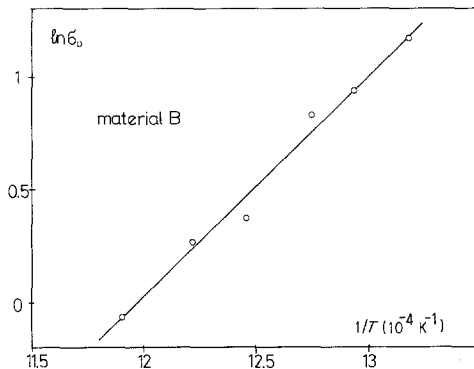


Figure 9 Determination of the activation energy of the threshold stress (material B). $Q_0 = 82 \text{ kJ mol}^{-1}$.

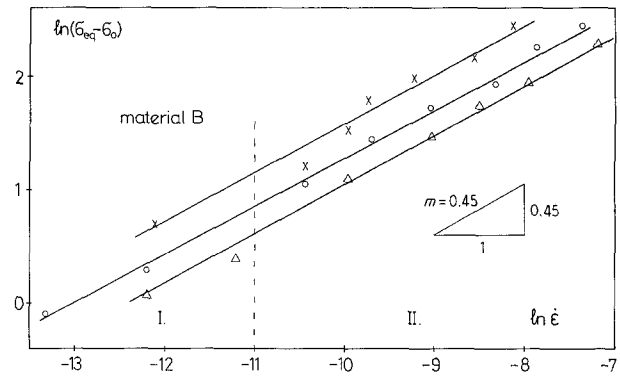


Figure 10 The effective stress-strain rate relationship for material B. $T = (\times)$ 785, (\circ) 803, (Δ) 818 K.

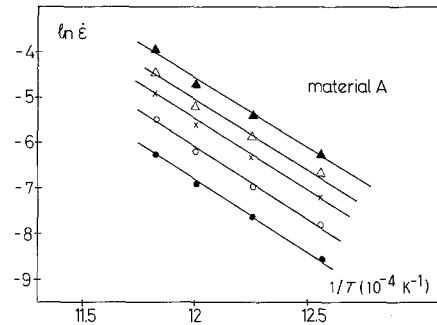


Figure 11 Determination of the apparent activation enthalpy (material A). $Q_a = 220 \text{ kJ mol}^{-1}$.

activation enthalpy of the superplastic processes in Al-33% Cu alloy is rather higher than the self-diffusion energy of the aluminium [14]. It is also well known, that for dispersionally strengthened alloys the activation enthalpy of the normal creep processes are higher than that of the self diffusion [15]. The results of the present investigation show that the high activation enthalpy of the alloys tested cannot be attributed solely to the existence of a temperature-dependent threshold stress. In the case of alloys containing dispersionally distributed precipitates which are coherent with the matrix, the activation enthalpy of the deformation nearly agrees with that of the bulk diffusion. On the contrary, if the precipitates are incoherent with the matrix, the activation enthalpy exceeds this value. In our case there are incoherent precipitates at the grain boundaries, therefore it is rather probable that the precipitations containing chromium and copper are the dominant factors in the development of the superplastic process.

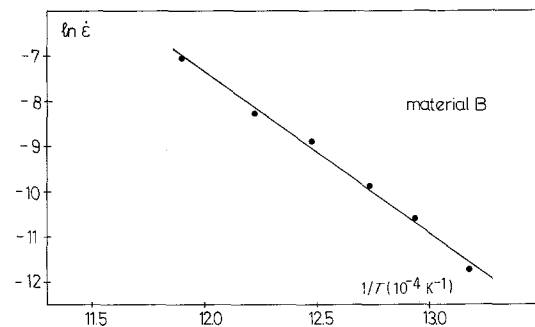


Figure 12 Determination of the apparent activation enthalpy (material B). $Q_a = 292 \text{ kJ mol}^{-1}$.

4. Conclusions

AlZnMg alloys were investigated by impression creep testing. The results show that in a suitable temperature and strain rate range the deformation is superplastic. Supposing a strongly temperature-dependent threshold stress, the first two regions of the deformation process can be interpreted on the basis of the same controlling micromechanism. However, the activation enthalpy obtained is higher than that of the bulk diffusion.

References

1. J. L. MARTIN, in "Creep Behaviour of Crystalline Solids, Progress in Creep and Fractures", edited by B. Wilshire and R. W. Evans (Pineridge Press, Swansea, UK, 1985) p. 1.
2. H. OIKAWA and T. G. LANGDON, *ibid.*, p. 33.
3. McLEAN, *Acta Metall.* **33** (1985) 545.
4. B. BURTON, "Diffusional Creep of Polycrystalline Materials, Diffusion and Defect Monograph Series" (Trans. Tech., Switzerland, 1977) p. 73.
5. J. H. GITTUS, in "Mechanics of Solids", edited by H. G. Hopkins and M. J. Sewell (Pergamon Press, London, 1982) p. 227.
6. T. G. LANGDON, *Met. Trans.* **13A** (1982) 689.
7. F. A. MOHAMED, *J. Mater. Sci. Lett.* **7** (1988) 215.
8. A. JUHÁSZ, N. Q. CHINH, P. TASNÁDI, P. SZÁSZVÁRI and L. KOVÁCS, "Materials Science Forum", Vol. 13/14, edited by I. Kovács and J. Lendvai (Trans. Tech., Switzerland, 1987) p. 421.
9. H. Y. YU, M. A. IMAM and B. B. RATH, *J. Mater. Sci.* **20** (1985) 636.
10. T. G. LANGDON and F. A. MOHAMED, *Scripta Metall.* **11** (1977) 575.
11. P. TASNÁDI, A. JUHÁSZ, N. Q. CHINH and I. KOVÁCS, *Res. Mech.* **24** (1988) 335.
12. A. JUHÁSZ, P. TASNÁDI, P. SZÁSZVÁRI and I. KOVÁCS, *J. Mater. Sci.* **21** (1986) 3287.
13. A. JUHÁSZ, N. Q. CHINH, R. TASNÁDI, I. KOVÁCS and T. TURMEZEY, *ibid.* **22** (1987) 137.
14. B. P. KASHYAP and K. TANGRI, *Scripta Metall.* **19** (1985) 1419.
15. E. ARTZ, M. F. ASHBY and R. A. VERRALL, *Acta Metall.* **31** (1983) 1977.

Received 5 June
and accepted 23 October 1989